Theory of femtosecond photon echoes in solid solutions

I. S. Osad'ko and M. V. Stashek

Moscow State Pedagogical University, 119882 Moscow, Russia

(Submitted 29 March 1994)
Zh. Eksp. Teor. Fiz. **106**, 535–552 (August 1994)

Formulas describing two- and three-pulse echo signal decay in doped systems are derived. For delays $\tau<1$ ps, this decay is nonexponential. This reflects the nonexponential nature of the ultrafast phase relaxation of electron dipoles due to the processes of phonon creation and annihilation. A quantitative relation is established between the echo decay law and the shape of the phonon limb of the homogeneous optical band of an impurity center. Femtosecond photon echoes are shown to provide data on the phonon spectrum of the system and electron–phonon interactions even in cases when zero-phonon lines are absent and other methods of selective spectroscopy are inapplicable.

1. INTRODUCTION

The photon echo is the optical analog of the spin echo.[1] It was therefore described using the Bloch equations in the first treatments[2,3] and in subsequent ones.[4,5] It follows from these equations that the pulse train shown in Fig. 1 generates a two-pulse (2PE) or three-pulse (3PE) photon echo signal. The echo amplitude depends exponentially on the delay τ.[5]

$$E_{2\mathrm{PE}}\propto\exp\left(-\frac{2\tau}{T_2}\right),\quad E_{3\mathrm{PE}}\propto\exp\left(-\frac{2\tau}{T_2}-\frac{t_w}{T_1}\right). \tag{1}$$

Both relaxation constants T_1 and T_2 appearing in the Bloch equations enter into Eqs. (1). They describe relaxation of the spin or atomic population (T_1) and phase relaxation (T_2). Experiments show that Eqs. (1) describe the situation adequately over a wide range of delays τ: from microseconds in microwave echo[6] to picoseconds in organic doped systems.[7]

The exponential formulas (1) are used even when $\ln E$ depends nonlinearly on τ.[8] This nonlinearity arises because T_2 depends on τ and is attributed to the spectral diffusion effect.[9] Spectral diffusion has been observed in both spin systems[8] and optical transitions of impurity centers of polymers.[10,11] It is usually explained by random variation of the spin or molecular resonant frequency in the process of the experiment.

The simple formulas (1) become inapplicable if the delay τ is shorter than several picoseconds. Experiments show that the echo signal decay on femtosecond[12,13] and even subpicosecond[14] time scales of τ becomes nonexponential and even can exhibit oscillations. This means that electron dipole phase relaxation is not purely exponential on the femtosecond time scale.

This behavior of ultrafast phase relaxation of impurity centers can be understood qualitatively if we turn not to photon echo but to a simpler coherent effect, polarization decay induced by a single optical pulse. It is known[9] that the function $I(t)$ describing the decay of this polarization is related to the optical band form function $I(\omega)$ through a Fourier transformation:

$$I(t)=\int_{-\infty}^{\infty}d\omega e^{-i\omega t}I(\omega). \tag{2}$$

The optical band $I(\omega)$ of an impurity center has a complicated shape. It consists of a narrow zero-phonon line of Lorentzian shape and a broad phonon limb corresponding to electron–phonon phototransitions.[15] Using a well-known property of Fourier transformation, we can conclude that the band shape in the region of small frequencies, i.e., in the zero-phonon line region, determines the behavior of the function $I(t)$ at large t, and the band shape in the high-frequency region i.e., in the phonon limb region, determines $I(t)$ at small t. Indeed, the exponential decay time T_2 of a polarization-induced signal is related to the half-width γ of the Lorentzian zero-phonon line through the simple formula

$$1/T_2=\gamma/2, \tag{3}$$

following from (2). But the intensity distribution in the phonon limb has a complicated character, since it reflects the phonon state density of the solid and the model of the interaction of an impurity center with phonons.[15] Therefore, the shape of the phonon limb cannot be Lorentzian, and the function $I(t)$ cannot be exponential at small t.

The phonon echo is a more complicated phenomenon than the phenomenon of polarization decay considered above, so the relation between the function $E(\tau)$ describing echo decay and the optical band form function $I(\omega)$ is more complicated. However, it exhibits the same behavior: electron–phonon transitions forming the phonon limb make the decay of the echo signal nonexponential at short times. At 4.2 K the homogeneous half-width γ of the zero-phonon line is no more than several gigahertz, which corresponds to T_2 of tens of picoseconds and more. The phonon wing half-width is no less than ten inverse centimeters corresponding to relaxation time a few hundreds of femtoseconds or less. Since the Bloch optical equations ignore the existence of the phonon limb, they cannot serve as a basis for treating femtosecond echoes.

Existing theoretical approaches to the problem of femtosecond echo calculation can be divided into two groups. The approaches belonging to the first group make use of the four-wave mixing method developed to treat various nonlinear

1063-7761/94/080293-10$10.00

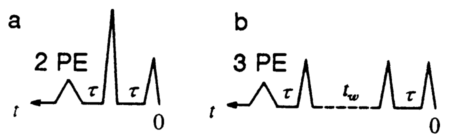

FIG. 1. Optical pulse train resulting in the appearance of two- (a) and three- (b) pulse echo.

spectroscopic phenomena.[16] This method employs a classical electromagnetic field. Echoes in electron-hole transitions in semiconductors,[17] in transitions between a discrete level and a band,[18] in electron-magnon systems,[19] and in electron–phonon systems[20–22] were analyzed by this method.

The approaches of the second group make use of quantum treatment of electromagnetic field. They attempt to go from four Bloch equations to an infinite-dimensional set of equations for a complete vibronic system. It was in precisely this way that a set of equations allowing for spontaneous processes determining the time T_1 (T_1-processes) and the fact that an optical band consists of a zero-phonon line and a phonon limb was recently derived.[23] Using this set of equations, we were able to treat photon echo signal decay.[24,25]

Each of these methods has its own advantages and disadvantages. The four-wave mixing method uses a classical electromagnetic field, so it does not take T_1-processes into account. Thus, this method gives an inaccurate expression for the amplitude $E_{3\mathrm{PE}}$. By contrast, the method developed in Refs. 23–25 includes T_1-processes but neglects a number of off-diagonal elements of the density matrix of a vibronic system. Such neglect is admissible in considering $E_{3\mathrm{PE}}$ but is invalid in considering $E_{2\mathrm{PE}}$.

The theory presented in this paper combines the advantages of both the methods mentioned. On the one hand, it allows for T_1-processes; on the other, the excitation field is treated classically, which greatly simplifies the theory and makes it possible to allow for nonmonochromatic exciting light. The latter is of extreme importance, since ultrashort laser pulses cannot be monochromatic by virtue of the uncertainty relation $\Delta\omega\Delta t \geqslant 1$.

2. EQUATION FOR THE DENSITY MATRIX OF A VIBRONIC SYSTEM

If short laser pulses with an optical frequency falling within the absorption domain of an impurity center pass through a sample containing such centers, the centers are polarized following pulse transmission:

$$\mathbf{P}_n(t) = \mathrm{Sp}[\hat{\mathbf{P}}_n \hat{\rho}(t)], \tag{4}$$

where $\mathbf{P}_n$ is the dipole moment operator of the nth center and $\hat{\rho}(t)$ is the density operator of the system. The operator $\hat{\rho}(t)$ satisfies the equation

$$i\hbar\dot{\hat{\rho}}(t) = [\hat{H}(t), \hat{\rho}], \tag{5}$$

where

$$\hat{H}(t) = \hat{H}_0 + \hat{\Lambda}(t) \tag{6}$$

is the Hamiltonian of the system. It includes the Hamiltonian $\hat{H}_0$ of the impurity center interacting with phonons and the interaction

$$\hat{\Lambda}(t) = \hat{\mathbf{P}}_n \mathbf{E}(n,t) \tag{7}$$

between the impurity center and the classical electromagnetic field.

We take the Hamiltonian of the electron-phonon system in the following form:

$$\hat{H}_0 = (\hbar\omega_0 + \hat{V})B^+B + \hat{H}^g. \tag{8}$$

Here, B^+ and B are the creation and annihilation operators of an electron excitation with energy $\hbar\omega_0$ in the nth impurity center, and $\hat{H}^g$ and $\hat{H}^e = \hat{H}^g + \hat{V}$ are adiabatic Hamiltonians obtained by averaging the total Hamiltonian over the electron states g and e describing unexcited and excited impurity centers.

The eigenfunctions of the individual terms in (8) are determined from the following equations:

$$\begin{aligned} &B^+B|0\rangle = 0, \quad B^+B|1\rangle = |1\rangle; \\ &H^g|\alpha\rangle = \epsilon_\alpha|\alpha\rangle, \quad H^e|\beta\rangle = \epsilon_\beta|\beta\rangle. \end{aligned} \tag{9}$$

Here ϵ_α and ϵ_β are the energies of low-frequency excitations of a medium for unexcited (ϵ_α) and excited (ϵ_β) impurity centers. In a crystal such excitations are phonons. Then $\langle\alpha|\beta\rangle$ is the Franck–Condon overlap integral of the oscillatory functions. In polymers and glasses, additional excitations exist along with phonons which correspond to tunnel transitions in so called two-level systems.[26,27] In this case, $\langle\alpha|\beta\rangle$ can also represent the overlap integral of the wave functions of such two-level systems. The effect of the two-level systems on the optical band shape has been considered recently in Refs. 28 and 29.

Evidently the eigenfunctions of the Hamiltonian H_0 will be of two types

$$|\alpha\rangle\rangle = |0\rangle|\alpha\rangle, \quad |\beta\rangle\rangle = |1\rangle|\beta\rangle. \tag{10}$$

In the basis consisting of these functions, Eq. (5) for the density operator $\hat{\rho}$ becomes the following set of equations:

$$\begin{aligned} i\dot{\rho}_{\beta\alpha} &= \omega_{\beta\alpha}\rho_{\beta\alpha} + \sum_{\alpha''} \Lambda_{\beta\alpha''}(t)\rho_{\alpha''\alpha} - \sum_{\beta''} \rho_{\beta\beta''}\Lambda_{\beta''\alpha}(t), \\ i\dot{\rho}_{\alpha\beta} &= \omega_{\alpha\beta}\rho_{\alpha\beta} + \sum_{\beta''} \Lambda_{\alpha\beta''}(t)\rho_{\beta''\beta} - \sum_{\alpha''} \rho_{\alpha\alpha''}\Lambda_{\alpha''\beta}(t), \\ i\dot{\rho}_{\beta\beta'} &= \omega_{\beta\beta'}\rho_{\beta\beta'} + \sum_{\alpha} \Lambda_{\beta\alpha}(t)\rho_{\alpha\beta'} - \sum_{\alpha} \rho_{\beta\alpha}\Lambda_{\alpha\beta'}(t), \\ i\dot{\rho}_{\alpha\alpha'} &= \omega_{\alpha\alpha'}\rho_{\alpha\alpha'} + \sum_{\beta} \Lambda_{\alpha\beta}(t)\rho_{\beta\alpha'} - \sum_{\beta} \rho_{\alpha\beta}\Lambda_{\beta\alpha'}(t), \end{aligned} \tag{11}$$

where

$$\begin{aligned} &\omega_{\beta\alpha} = \omega_0 + \frac{\varepsilon_\beta - \varepsilon_\alpha}{\hbar}, \quad \omega_{\beta\beta'} = \frac{\varepsilon_\beta - \varepsilon_{\beta'}}{\hbar}, \\ &\omega_{\alpha\alpha'} = \frac{\varepsilon_\alpha - \varepsilon_{\alpha'}}{\hbar}, \quad \Lambda_{\beta\alpha}(t) = \left\langle \beta \left| \frac{\Lambda(t)}{\hbar} \right| \alpha \right\rangle. \end{aligned} \tag{12}$$

If we neglect the elements $\rho_{\beta\beta'}$ and $\rho_{\alpha\alpha}$ with $\beta\neq\beta'$ and $\alpha\neq\alpha'$, the set of equations (11) is transformed into the set (5) of Ref. 23, where the exciting electromagnetic field was treated quantum mechanically. There are only two differences: in Eqs. (11) the frequencies $\omega_{\beta\alpha}$ and $\omega_{\alpha\beta}$ do not contain the phonon frequency, and the matrix elements $\Lambda_{\beta\alpha}$ are time-dependent. These distinctions are not fundamental, as the system (11) simplified in the manner described above can be rearranged into the system (5) of Ref. 23 when the external excitation is monochromatic.

The set of equations (11) does not include spontaneous light emission processes. To include them we should extend the basis (10) by taking the following set of functions:

$$|0\rangle|\alpha\rangle,\quad |1\rangle|\beta\rangle,\quad |0\rangle|1_k\rangle|\alpha\rangle,\quad |1\rangle|1_k\rangle|\beta\rangle,$$
$$|0\rangle|1_k1_{k'}\rangle|\alpha\rangle,\quad |1\rangle|1_k1_{k'}\rangle|\beta\rangle,\ldots,$$

where $|v_k\rangle$ is the harmonic oscillator function describing v photons in the mode k. Instead of the set of equations (11), a more complicated set of equations for density matrix elements depending on the indices α and β as well as on the indices k of spontaneously emitted photons appears in this basis. Reference 23 shows how to pass from the set of equations for the complete density matrix containing the indices k of the emitted phonons to the set of equations for the reduced matrix whose elements are traces over all possible quantum states of the emitted photons. Matrix elements reduced in this way no longer depend on the indices k, and the set of equations for the reduced elements will appear as follows:

$$\begin{aligned}
i\dot{\rho}_{\beta\alpha}&=\left(\omega_{\beta\alpha}-\frac{i}{2T_1}\right)\rho_{\beta\alpha}+\sum_{\alpha''}\Lambda_{\beta\alpha''}(t)\rho_{\alpha''\alpha}\\
&\quad-\sum_{\beta''}\rho_{\beta\beta''}\Lambda_{\beta''\alpha}(t),\\
i\dot{\rho}_{\alpha\beta}&=\left(\omega_{\alpha\beta}-\frac{i}{2T_1}\right)\rho_{\alpha\beta}+\sum_{\beta''}\Lambda_{\alpha\beta''}(t)\rho_{\beta''\beta}\\
&\quad-\sum_{\alpha''}\rho_{\alpha\alpha''}\Lambda_{\alpha''\beta}(t),\\
i\dot{\rho}_{\beta\beta'}&=(\omega_{\beta\beta'}-i\Gamma)\rho_{\beta\beta'}+\sum_{\alpha}\Lambda_{\beta\alpha}(t)\rho_{\alpha\beta'}\\
&\quad-\sum_{\alpha}\rho_{\beta\alpha}\Lambda_{\alpha\beta'}(t),\\
i\dot{\rho}_{\alpha\alpha'}&=\omega_{\alpha\alpha'}\rho_{\alpha\alpha'}+\sum_{\beta}\Lambda_{\alpha\beta}(t)\rho_{\beta\alpha'}-\sum_{\beta}\rho_{\alpha\beta}\Lambda_{\beta\alpha'}(t)\\
&\quad+i\sum_{\beta\beta'}\langle\alpha|\beta\rangle\,\frac{\rho_{\beta\beta'}}{T_1}\,\langle\beta'|\alpha'\rangle.
\end{aligned}\tag{13}$$

The elimination of spontaneously emitted photons using the reduction operation results in the appearance of the relaxation constant T_1. In the derivation of the set of equations (13), we also took into account the fact that a photochemical reaction with a rate Q occurs in the excited electron state of an impurity center. Therefore, the constant $\Gamma=1/T_1+Q$ appears. The set of equations (13) is valid also for arbitrary nonmonochromatic classical electromagnetic field, i.e., for arbitrary dependence of $\Lambda_{\beta\alpha}$ on t, because the spectral composition of the exciting light has no effect on spontaneous transitions described by the time T_1.

3. FORMAL SOLUTION OF SYSTEM (13)

The set of equations (13) may be rewritten in the following form

$$i\dot{\rho}=[\hat{\varepsilon}+\hat{\Lambda}(t)]\rho,\tag{14}$$

where ρ is the infinite-dimensional Bloch vector, which may be written symbolically in the form

$$\rho(t)=\begin{pmatrix}\rho_{\beta\alpha}(t)\\ \rho_{\alpha\beta}(t)\\ \rho_{\beta\beta'}(t)\\ \rho_{\alpha\alpha'}(t)\end{pmatrix}.\tag{15}$$

The matrix $\hat{\varepsilon}$ is obtained from Eqs. (13) if all $\Lambda_{\alpha\beta}$ and $\Lambda_{\beta\alpha}$ are set equal to zero in the latter. The matrix $\hat{\Lambda}(t)$ describes pumping.

Integrating Eq. (14), we arrive at the following integral equation

$$\rho(t)=\rho_0(t)-i\int_{-\infty}^{t}dt'\ \exp[-i\hat{\varepsilon}(t-t')]\hat{\Lambda}(t')\rho(t'),\tag{16}$$

where

$$\rho_0(t)=\exp(-i\hat{\varepsilon}t)\rho(-\infty).\tag{17}$$

It can be seen that at $t=-\infty$, we have

$$\rho(-\infty)=\begin{pmatrix}0\\0\\0\\ \rho_{\alpha\alpha}(-\infty)\end{pmatrix}.\tag{18}$$

In the absence of pumping the population $\rho_{\alpha\alpha}(-\infty)$ has its equilibrium value and cannot evolve with time, i.e., $\rho_0(t)=\rho(-\infty)$. Solving Eq. (16) by iteration, we find

$$\rho(t)=\rho_0+\rho_1(t)+\rho_2(t)+\rho_3(t)+\ldots\ ,\tag{19}$$

where

$$\begin{aligned}
\rho_1(t)&=-i\int_{-\infty}^{t}dt'\ \exp[-i\hat{\varepsilon}(t-t')]\hat{\Lambda}(t')\rho(-\infty),\\
\rho_2(t)&=(-i)^2\int_{-\infty}^{t}dt'\int_{-\infty}^{t'}dt''\ \exp[-i\hat{\varepsilon}(t-t')]\\
&\quad\times\hat{\Lambda}(t')\exp[-i\hat{\varepsilon}(t'-t'')]\hat{\Lambda}(t'')\rho(-\infty),\\
\rho_3(t)&=(-i)^3\int_{-\infty}^{t}dt'\int_{-\infty}^{t'}dt''\int_{-\infty}^{t''}dt'''\ \exp[-i\hat{\varepsilon}(t-t')]\\
&\quad\times\hat{\Lambda}(t')\exp[-i\hat{\varepsilon}(t'-t'')]\hat{\Lambda}(t'')\exp[-i\hat{\varepsilon}(t''-t''')]\\
&\quad\times\hat{\Lambda}(t''')\rho(-\infty).
\end{aligned}\tag{20}$$

The vector $\rho_1(t)$ allows us to find the behavior of the sample polarization induced by light to first order in $\hat{\Lambda}$:

$$P_1(t)=\mathrm{Sp}\sum_n \hat{P}_n\rho_1(t). \tag{21}$$

The vector $\rho_2(t)$ allows the evolution of the molecular level populations to be found to lowest order in $\hat{\Lambda}$:

$$n_g(t)=\sum_\alpha \rho_2(t)_{\alpha\alpha},\quad n_e(t)=\sum_\beta \rho_2(t)_{\beta\beta}. \tag{22}$$

Finally, the vector $\rho_3(t)$ makes it possible to find both the third-order correction in $\hat{\Lambda}$ to the induced polarization signal and the photon echo signal amplitude:

$$P_3(t)=\mathrm{Sp}\sum_n \hat{P}_n\rho_3(t). \tag{23}$$

This is the starting formula for the following calculations.

4. TRANSFORMATION OF THE FORMULA FOR $P_3(t)$

Substituting the expression for $\rho_3(t)$ in Eq. (23), we find

$$P_3(t)=i\int_{-\infty}^{t}dt_1\int_{-\infty}^{t_1}dt_2\int_{-\infty}^{t_2}dt_3\ \mathrm{Sp}\sum_n \{\hat{P}_n \exp[-i\hat{\varepsilon}$$
$$\times(t-t_1)]\hat{\Lambda}(t_1)\exp[-i\hat{\varepsilon}(t_1-t_2)]\hat{\Lambda}(t_2)$$
$$\times\exp[-i\hat{\varepsilon}(t_2-t_3)]\hat{\Lambda}(t_3)\rho(-\infty)\}. \tag{24}$$

Let the electric field in the operator $\hat{\Lambda}(t)$ depend on time in the manner shown in Fig. 1b. We assume that all three pulses propagate in the same direction. Then the electric field of each pulse is described by

$$\mathbf{E}(n,t)=\sum_k \mathbf{E}_k \exp\left[-ikc\left(t-\frac{n}{c}\right)\right]+\text{c.c.} \tag{25}$$

Here n is the impurity center coordinate in the direction of ray propagation. The simplest expression for P_3 is obtained for $\Delta t\ll\tau$, where Δt is the pulse length. In this case we may assume that the pulse is a δ-function:

$$\mathbf{E}(n,t)=\mathbf{E}\delta\left(t-\frac{n}{c}\right). \tag{26}$$

In this case the operator $\hat{\Lambda}(t)$ takes the form

$$\hat{\Lambda}(t)=\hat{\Lambda}_n\left[\delta\left(t-\frac{n}{c}\right)+\delta\left(t-\tau-\frac{n}{c}\right)+\delta\left(t-\tau-t_w-\frac{n}{c}\right)\right], \tag{27}$$

where $\hat{\Lambda}_n=\hat{\mathbf{P}}_n\mathbf{E}$ is a time-independent operator. Taking into account the inequatities $t_3<t_2<t_1<t$, we may substitute the following expressions in formula (24):

$$\hat{\Lambda}(t_1)=\hat{\Lambda}_n\delta\left(t_1-\tau-t_w-\frac{n}{c}\right),$$
$$\hat{\Lambda}(t_2)=\hat{\Lambda}_n\delta\left(t_2-\tau-\frac{n}{c}\right),$$
$$\hat{\Lambda}(t_3)=\hat{\Lambda}_n\delta\left(t_3-\frac{n}{c}\right). \tag{28}$$

Noting that $f(x)\delta(x-x_0)=f(x_0)\delta(x-x_0)$, we find the following expression after substitution of (28) in (24):

$$P_3(t)=i\ \mathrm{Sp}\sum_n \left\{\hat{P}_n \exp\left[-i\hat{\varepsilon}\left(t-\tau-t_w-\frac{n}{c}\right)\right]\right.$$
$$\left.\times\hat{\Lambda}_n \exp(-i\hat{\varepsilon}t_w)\hat{\Lambda}_n \exp(-i\hat{\varepsilon}\tau)\hat{\Lambda}_n\rho(-\infty)\right\}$$
$$\times\int_{-\infty}^{t}dt_1\delta\left(t_1-\tau-t_w-\frac{n}{c}\right)\int_{-\infty}^{t_1}dt_2\delta\left(t_2-\tau-\frac{n}{c}\right)$$
$$\times\int_{-\infty}^{t_2}dt_3\delta\left(t_3-\frac{n}{c}\right). \tag{29}$$

Evaluating the integral, we get the Heaviside step function $\theta(t-\tau-t_w-n/c)$, i.e., P_3 is nonzero only if $t>\tau+t_w+n/c$. Introducing $\tau'=t-\tau-t_w-n/c$, we can represent (29) in the following form:

$$P_3=i\ \mathrm{Sp}\sum_n [\hat{P}_n \exp(-i\hat{\varepsilon}\tau')\hat{\Lambda}_n \exp(-i\hat{\varepsilon}t_w)\hat{\Lambda}_n$$
$$\times\exp(-i\hat{\varepsilon}\tau)\hat{\Lambda}_n\rho(-\infty)]. \tag{30}$$

The farther the molecule n is located down the ray path, the later polarization develops in it.

5. FORMULAS FOR THE ECHO SIGNAL AMPLITUDE

The matrices in Eq. (30) are determined by means of Eqs. (13). Using Eqs. (13) and the initial condition (18), we readily find

$$\rho(\tau)=\exp(-i\hat{\varepsilon}\tau)\hat{\Lambda}_n\rho(-\infty)$$
$$=\begin{pmatrix}\exp(-i\Omega_{\beta\alpha}\tau)\Lambda_{\beta\alpha}\rho_{\alpha\alpha}\\ -\rho_{\alpha\alpha}\Lambda_{\alpha\beta}\exp(-i\Omega_{\alpha\beta}\tau)\\ 0\\ 0\end{pmatrix}=\begin{pmatrix}\rho_{\beta\alpha}(\tau)\\ \rho_{\alpha\beta}(\tau)\\ 0\\ 0\end{pmatrix}. \tag{31}$$

Here $\Lambda_{\beta\alpha}=\langle\beta|\alpha\rangle\Lambda_n$, where $\Lambda_n=\langle 0|\hat{\mathbf{P}}_n\mathbf{E}|1\rangle$ is the electron matrix element, and $\Omega_{\beta\alpha}=\omega_{\beta\alpha}-i/2T_1$. When the second pulse is transmitted, the vector $\rho(\tau)$ takes the form

$$\hat{\Lambda}_n\rho(\tau)=\begin{pmatrix}0\\ 0\\ \sum_{\alpha''}\Lambda_{\beta\alpha''}\rho_{\alpha''}\beta'(\tau)-\sum_{\alpha''}\rho_{\beta\alpha''}(\tau)\Lambda_{\alpha''\beta'}\\ \sum_{\beta''}\Lambda_{\alpha\beta''}\rho_{\beta''\alpha'}(\tau)-\sum_{\beta''}\rho_{\alpha\beta''}(\tau)\Lambda_{\beta''\alpha'}\end{pmatrix}$$
$$=\begin{pmatrix}0\\ 0\\ \rho_{\beta\beta'}(\tau)\\ \rho_{\alpha\alpha'}(\tau)\end{pmatrix}. \tag{32}$$

After a delay t_w the vector $\hat{\Lambda}_n\rho(\tau)$ assumes the form

$$\rho_3(t_w+\tau)=\exp(-i\hat{\varepsilon}t_w)\hat{\Lambda}_n\rho(\tau)=\begin{pmatrix} 0 \\ 0 \\ \exp(-i\Omega_{\beta\beta'}t_w)\rho_{\beta\beta'}(\tau) \\ \sum\limits_{\beta\beta'} M_{\alpha\alpha'\beta\beta'}(t_w)\rho_{\beta\beta'}(\tau)+\exp(-i\omega_{\alpha\alpha'}t_w)\rho_{\alpha\alpha'}(\tau) \end{pmatrix}=\begin{pmatrix} 0 \\ 0 \\ \rho_{\beta\beta'}(t_w+\tau) \\ \rho_{\alpha\alpha'}(t_w+\tau) \end{pmatrix}. \tag{33}$$

Here $\Omega_{\beta\beta'}=\omega_{\beta\beta'}-i\Gamma$, and the expression for the matrix $M_{\alpha\alpha'}\beta\beta'(t_w)$ can readily be found using the Eqs. (13). Setting all $\Lambda_{\alpha\beta}$ and $\Lambda_{\beta\alpha}$ in it equal to zero, and solving the resulting set of equations, we find

$$M_{\alpha\alpha'\beta\beta'}(t_w)=\frac{1}{T_1}\langle\alpha|\beta\rangle\langle\beta'|\alpha'\rangle\int_0^{t_w}dx\ \exp[i\omega_{\alpha\alpha'}(x-t_w)-i\Omega_{\beta\beta'}x]. \tag{34}$$

Finally, after the transmission of the third laser pulse and free relaxation for a time τ', the Bloch vector ρ takes the form

$$\rho(\tau'+t_w+\tau)=\exp(-i\hat{\varepsilon}\tau')\hat{\Lambda}_n\rho(t_w+\tau)=\begin{pmatrix} \exp(-i\Omega_{\beta\alpha}\tau')\left(\sum\limits_{\alpha'}\Lambda_{\beta\alpha'}\rho_{\alpha'\alpha}(t_w+\tau)-\sum\limits_{\beta'}\rho_{\beta\beta'}(t_w+\tau)\Lambda_{\beta'\alpha}\right) \\ \exp(-i\Omega_{\alpha\beta}\tau')\left(\sum\limits_{\beta'}\Lambda_{\alpha\beta'}\rho_{\beta'\beta}(t_w+\tau)-\sum\limits_{\alpha'}\rho_{\alpha\alpha'}(t_w+\tau)\Lambda_{\alpha'\beta}\right) \\ 0 \\ 0 \end{pmatrix}$$

$$=\begin{pmatrix} \rho_{\beta\alpha}(\tau'+t_w+\tau) \\ \rho_{\alpha\beta}(\tau'+t_w+\tau) \\ 0 \\ 0 \end{pmatrix}. \tag{35}$$

Substituting (35) in expression (30) for P_3, we find

$$P_3(\tau'+t_w+\tau)=\sum_{\alpha\beta}\sum_n[P_n^{\alpha\beta}\rho_{\beta\alpha}(\tau'+t_w+\tau)+P_n^{\beta\alpha}\rho_{\alpha\beta}(\tau'+t_w+\tau)], \tag{36}$$

where $P_n^{\alpha\beta}=\langle\alpha|\beta\rangle P_n$ and $P_n=i\langle 0|\hat{P}_n|1\rangle$ is the electron matrix element. The final expression for P_3 is obtained if we substitute (31) in (32), then (32) and (34) in (33), then (33) in (35), and finally (35) in (36). The resulting expression for P_3 will be rather cumbersome. There is no point in writing it out in full because by no means all the items constituting the expression for P_3 contribute to the photon echo. Thus, each item will contain a factor of either $\exp[\pm i\omega_0(\tau'-\tau)]$ or $\exp[\pm i\omega_0(\tau'+\tau)]$, where ω_0 is the electron dipole resonant frequency. The coefficients multiplying the complex conjugate exponentials will be complex conjugate as well. Equation (36) may therefore be written in the form

$$P_3(\omega_0)=2\ \mathrm{Re}\sum_n\{a_n(\tau',t_w,\tau)\exp[-i\omega_0(\tau'-\tau)]+b_n(\tau',t_w,\tau)\exp[-i\omega_0(\tau'+\tau)]\}. \tag{37}$$

Evidently, the amplitude $E_{3\mathrm{PE}}$ of the three-pulse echo signal is proportional to the total induced dipole moment of the sample:

$$E_{3\mathrm{PE}}\propto\int_{-\infty}^{\infty}d\omega_0P_3(\omega_0). \tag{38}$$

If we substitute (37) in (38) and integrate over frequency, we find

$$E_{3\mathrm{PE}}\propto 2\ \mathrm{Re}\sum_n a_n(\tau,t_w,\tau)\delta(\tau'-\tau). \tag{39}$$

The coefficients b_n vanish, since they are multiplied by the function $\delta(\tau'+\tau)$ which is zero since τ' and $\tau>0$.

The expression for $a_n(\tau,t_w,\tau)$ contains $\exp(\pm i\varepsilon_\alpha t/\hbar)$ and $\exp(\pm i\varepsilon_\beta t/\hbar)$. According to Eqs. (9), the energies ε_α and ε_β may be replaced by H^g and H^e, respectively. Using the property of completeness of the bases $|\alpha\rangle$ and $|\beta\rangle$, we arrive at the following expression for the function a_n:

$$a_n=P_n\Lambda_n^3R(\tau,t_w,\tau), \tag{40}$$

where

$$\begin{aligned}R(\tau,t_w,\tau)=\exp\left(-\frac{\tau}{T_1}\right)2\ \mathrm{Re}\Bigg\{&\mathrm{Sp}(\exp[-iH^e(\tau+t_w)]\\&\times\exp[-iH^g\tau]\hat{\rho}\exp[iH^e(\tau+t_w)]\\&\times\exp[iH^g\tau])\exp(-\Gamma t_w)\\&+\mathrm{Sp}(\exp[-iH^e\tau]\exp[-iH^g(t_w+\tau)]\hat{\rho}\\&\times\exp[iH^e\tau]\exp[iH^g(\tau+t_w)])\\&-\frac{1}{T_1}\int_0^{t_w}dx\ \exp(-\Gamma x)\mathrm{Sp}(\exp(-iH^e\tau)\\&\times\exp[iH^g(x-t_w)]\exp(-iH^ex)\hat{\rho}\\&\times\exp(-iH^g\tau)\exp[iH^e(x+\tau)]\end{aligned}$$

$$\left.\times\exp[iH^g(\tau-x+t_w)])\right\}. \tag{41}$$

Since the function $R(\tau,t_w,\tau)$ does not depend on the index n characterizing the position of a molecule, it is appropriate to represent Eq. (39) for $E_{3\mathrm{PE}}$ in the form

$$E_{3\mathrm{PE}}\propto R(\tau,t_w,\tau)\sum_n P_n\Lambda_n^3\delta(\tau'-\tau). \tag{42}$$

It is seen from Fig. 1 that by setting $t_w=0$, we arrive at the excitation mode typical of the two-pulse echo. Consequently,

$$E_{2\mathrm{PE}}\propto R(\tau,0,\tau)\sum_n P_n\Lambda_n^3\delta(\tau'-\tau). \tag{43}$$

Summation over n in Eqs. (42) and (43) determines the echo signal shape, and the functions $R(\tau,t_w,\tau)$ and $R(\tau,0,\tau)$ determine the amplitudes of three- and two-pulse echoes.

6. CALCULATION OF THE AMPLITUDE $R(\tau,t_w,\tau)$

Equation (41) enables one to consider the effect of both phonons and tunnel excitations of two-level systems present in polymers and glasses on the photon echo signal. In this paper, we restrict ourselves to allowing for electron–phonon interaction only. This interaction contains parts linear and quadratic in the phonon coordinates $\mathbf{R}$. According to the theory of Refs. 15 and 30, the quadratic interaction determines thermal broadening of a zero-phonon line and only weakly affects the shape and intensity of the phonon limb, which is determined predominantly by the linear Franck–Condon interaction.[30] Since it is the phonon limb that determines phase relaxation on femtosecond time scales, we neglect the quadratic Franck–Condon interaction and set

$$H^g=H(\mathbf{R}),\quad H^e=H(\mathbf{R}-\mathbf{a}), \tag{44}$$

where $H(\mathbf{R})$ is the Hamiltonian of the harmonic oscillator. Equations (44) include only linear interaction appearing due to the shifts of oscillator equilibrium positions. In this case, using the translation operator $\exp(\mathbf{a}\boldsymbol{\nabla})$, we find

$$\exp[iH(\mathbf{R}-\mathbf{a})t]=\exp[-(\mathbf{a}\boldsymbol{\nabla})]\exp[iH(\mathbf{R})t]\exp(\mathbf{a}\boldsymbol{\nabla}). \tag{45}$$

The transformation (45) allows us to rearrange all the operators H^e into the operators $H^g=H$ in formula (41). The procedure for calculating expressions similar to those appearing in (41) is described in Ref. 30. The result of evaluating (41) is the following:

$$\begin{aligned}R(\tau,t_w,\tau)={}&\exp\left(-\frac{\tau}{T_1}\right)2\,\mathrm{Re}\Bigg\{\exp[2g(\tau)+g_1(\tau,t_w)\\&-\Gamma t_w]+\exp[2\,\mathrm{Re}\,g(\tau)]\Bigg[\exp[g_2(\tau,t_w)]\\&-\exp[g_1(\tau,t_w)-\Gamma t_w]\,\frac{1}{T_1}\int_0^{t_w}dx\,\exp\{\Gamma x\\&-2i\,\mathrm{Im}[g(\tau+x)-g(x)]\}\Bigg]\Bigg\},\end{aligned} \tag{46}$$

where

$$\begin{aligned}g_1&=-g^*(t_w)+2\,\mathrm{Re}\,g(\tau+t_w)-g(2\tau+t_w),\\g_2&=-g(t_w)+2g(\tau+t_w)-g(2\tau+t_w).\end{aligned} \tag{47}$$

The essential feature of formula (46) is that the echo signal amplitude is expressed in terms of a single function

$$\begin{aligned}g(\tau)=\sum_\xi\left(\frac{a_\xi}{2}\right)^2&[(n_\xi+1)\exp(-i\nu_\xi\tau)+n_\xi\exp(i\nu_\xi\tau)\\&-(2n_\xi+1)],\end{aligned} \tag{48}$$

which contains all information on phonons and the electron–phonon interaction. Here ν_ξ is the phonon frequency, a_ξ is the shift of the ξth normal coordinate, and $n_\xi=[\exp(\hbar\nu_\xi/kT)-1]^{-1}$.

7. ANALYSIS OF THE FUNCTION $g(t)$

From the formula (48) an obvious property of the function g follows: $g(-t)=g^*(t)$. It is appropriate to write (48) in the following form:

$$g(\tau)=f(\tau,T)-f(0,T), \tag{49}$$

where

$$\begin{aligned}f(\tau,T)={}&\int_{-\infty}^{\infty}d\nu[(n(\nu)+1)f(\nu)+n(-\nu)f(-\nu)]\\&\times\exp[-i\nu\tau]=\int_{-\infty}^{\infty}d\nu f(\nu,T)\exp[-i\nu\tau],\end{aligned} \tag{50}$$

$$f(\nu)=\sum_\xi\left(\frac{a_\xi}{2}\right)^2\delta(\nu-\nu_\xi). \tag{51}$$

Here $n(\nu)=[\exp(\hbar\nu/kT)-1]^{-1}$. The function $f(\nu)$ determines the density of phonon states weighted with the coupling function $(a_\xi/2)^2$. The vanishing of this function at a frequency ν_0 means that either phonons with a frequency ν_0 are absent in the solid or such phonons do not interact with electrons.

The function $f(\tau,T)$ determines the shape of the phonon limb in the optical band, and the constant $f(0,T)$ is called the Pekar–Huang factor. It is known[30] that the functions $I^{g,e}(\omega)$ of the homogeneous absorption (g) and fluorescence (e) band shapes are very easily expressed in terms of the function $g(t)$

$$I^{g,e}(\omega)=\frac{1}{2\pi}\int_{-\infty}^{\infty}dt\,\exp[i(\omega-\omega_0)t+g(\pm t)]. \tag{52}$$

Substituting (48) here, expanding $\exp[f(t,T)]$ in a series in $f(t,T)$, and integrating the terms of the series over time, we find

$$I^{g,e}(\omega)=\exp[-f(0,T)]\left[\delta(\omega-\omega_0)+\sum_{n=1}^{\infty}\Phi_n^{g,e}(\omega-\omega_0)\right], \tag{53}$$

where

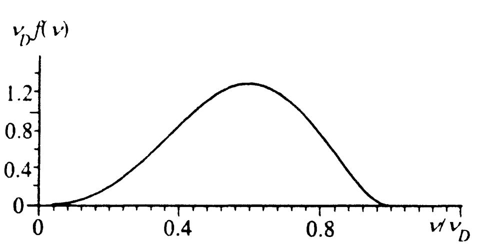

FIG. 2. The function of weighted phonon state density whose integral value $f(0,0)$ is 0.625.

$$\Phi_n^g(\omega-\omega_0)=\frac{1}{n!}\int_{-\infty}^{\infty}d\nu_1\ldots\int_{-\infty}^{\infty}d\nu_n f(\nu_1,T)\ldots f(\nu_n,T)\,\delta(\omega-\omega_0-\nu_1-\ldots-\nu_n), \tag{54}$$

and $\Phi_n^e(\omega-\omega_0)=\Phi_n^g(\omega_0-\omega)$. Evidently the δ-function in formula (53) describes a zero-phonon line, and the function $\exp[-f(0,T)]\Phi_n$ determines the probability of phototransitions with creation and annihilation of n photons. Zero-phonon lines of absorption and fluorescence are resonant with one another, and the phonon limbs of both lines are mirror-symmetrical with respect to the zero-phonon line.

As a simple example, we consider the case when an impurity center interacts with acoustic vibrations of a solid. We take the function $f(\nu)$ in the quasi-Debye form

$$f(\nu)=\begin{cases} f_0\left(\frac{\nu}{\nu_D}\right)^3\left(1-\frac{\nu}{\nu_D}\right)^2, & \nu\leqslant\nu_D,\\ 0, & \nu>\nu_D,\end{cases} \tag{55}$$

where ν_D is the threshold frequency of acoustic phonons. The function (55) is depicted in Fig. 2. Using (49) and (50), we find

$$\operatorname{Re} g(\tau)=\operatorname{Re} f(\tau,T)-f(0,T), \quad \operatorname{Im} g(\tau)=-\operatorname{Im} f(\tau), \tag{56}$$

where

$$\operatorname{Re} f(\tau,T)=\int_0^{\infty}d\nu f(\nu)\coth\frac{\hbar\nu}{2kT}\cos\nu\tau,$$

$$\operatorname{Im} f(\tau)=\int_0^{\infty}d\nu f(\nu)\sin\nu\tau. \tag{57}$$

The functions $\operatorname{Re} f$ and $\operatorname{Im} f$ calculated by means of functions (55) and (57) at $T=0$ are presented in Fig. 3. These functions are nonmonotonic and decay over times of order $10\nu_D^{-1}$. Since in organic solids we have $\nu_D\sim 50$–$100\ \mathrm{cm}^{-1}$,[15] then $10\nu_D^{-1}\sim 1$–0.5 ps. Consequently, electron dipole phase relaxation resulting from acoustic phonon creation proceeds in a time less than one picosecond.

8. PHOTON ECHO SIGNALS

The general formula (46) for the relaxation function $R(\tau,t_w,\tau)$ is substantially simplified if we set $t_w=0$, i.e., turn to the consideration of two-pulse echo. In this case, the integral in formula (46) vanishes, and we find

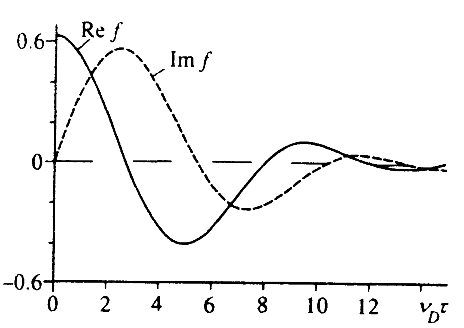

FIG. 3. Real and imaginary parts of the function $f(t,T)$ at $T=0$ calculated from Eqs. (57) with the function $f(\nu)$ shown in Fig. 2.

$$R(\tau,0,\tau)=\exp\left(-\frac{\tau}{T_1}\right)4\operatorname{Re}\{\exp[2g(\tau)+2\operatorname{Re} g(\tau)-g(2\tau)]\}. \tag{58}$$

This formula coincides with formula (19a) deduced earlier in Ref. 21. It is usual to set $t_w\sim T_1$ in studies of three-pulse echo decay laws. In this case the general formula (46) is also considerably simplified because all the functions g contained in the argument t_w tend to zero for $t_w\gg\nu_D^{-1}$ (see Fig. 3). Hence, $g_1=g_2=0$, and (46) takes the form

$$R(\tau,t_w,\tau)=\exp\left(-\frac{\tau}{T_1}\right)2\operatorname{Re}\left\{\exp[2g(\tau)-\Gamma t_w]+\exp[2\operatorname{Re} g(\tau)]\left[\frac{Q}{\Gamma}+\frac{1}{T_1\Gamma}\times\exp(-\Gamma t_w)\right]\right\}. \tag{59}$$

Using the formulas (56), we can express the functions $R(\tau,0,\tau)$ and $R(\tau,t_w,\tau)$ in terms of $\operatorname{Re} f(\tau)$ and $\operatorname{Im} f(\tau)$, shown in Fig. 3

$$R(\tau,0,\tau)=2\cos\{\operatorname{Im}[2f(\tau)-f(2\tau)]\}\exp\left\{-\frac{\tau}{T_1}+\operatorname{Re}[4f(\tau,T)-f(2\tau,T)]-3f(0,T)\right\}, \tag{60}$$

$$R(\tau,t_w,\tau)=\left\{\frac{Q}{\Gamma}+\left(\frac{1}{T_1\Gamma}+\cos[2\operatorname{Im} f(\tau)]\right)\times\exp(-\Gamma t_w)\right\}\exp\left[-\frac{\tau}{T_1}+\operatorname{Re} 2f(\tau,T)-2f(0,T)\right]. \tag{61}$$

The expression (61) coincides with Eq. (63) of Ref. 25. Recall that Eq. (63) of Ref. 25 was derived by means of a simplified set of equations which can be obtained from Eqs. (13) of this work if we discard $\rho_{\alpha\alpha'}$ and $\rho_{\beta\beta'}$ with $\alpha\neq\alpha'$ and $\beta\neq\beta'$ in it. Hence it follows that three-pulse echoes may be treated by dropping the elements that are nondiagonal in α and β in the set of equations (13).

Long delays τ

It follows from Fig. 3 that $\operatorname{Re} f$ and $\operatorname{Im} f=0$ if $\tau\nu_D>10$. If we take $\nu_D\sim 50\ \mathrm{cm}^{-1}$, then τ should exceed 1 ps. Neglecting photochemical transformations, i.e., assuming $Q=0$, we find using formulas (60) and (61) that

$$R(\tau,0,\tau)\propto\exp\left(-\frac{\tau}{T_1}\right),\qquad R(\tau,t_w,\tau)\propto\exp\left(-\frac{\tau}{T_1}-\frac{t_w}{T_1}\right). \tag{62}$$

The decrease in the echo signal is exponential, but the formulas (62) differ from (1) in that $1/2T_1$ appears in them instead of $1/T_2$. This distinction is easily explainable. Indeed, it follows from the Bloch equations that if the interaction with phonons results in a Lorentzian line shape with a half width γ, then[5,31]

$$\frac{1}{T_2}=\frac{\gamma}{2}+\frac{1}{2T_1}. \tag{63}$$

On the other hand, it is known[15,30] that the linear Franck–Condon interaction does not result in zero-phonon line broadening. It is only due to the quadratic interaction, which is neglected here. Consequently, in our theory we have $\gamma=0$, and so $1/T_2=1/2T_1$. As for the dependence on long delays t_w, it is identical in (62) and (1).

If we take into account the possibility of photochemical reaction in the excited state, then

$$R(\tau,t_w,\tau)=\exp\left(-\frac{\tau}{T_1}\right)\left[\frac{Q}{\Gamma}+\left(\frac{1}{T_1\Gamma}+1\right)\exp\left(-\frac{t_w}{T_1}\right)\right]. \tag{64}$$

Here, Q/Γ is the photochemical reaction quantum yield.

Short delays τ

If $\tau\nu_D<10$, then $\operatorname{Re} f$ and $\operatorname{Im} f\neq 0$. This takes place for $\tau<1$ ps. It is the functions $\operatorname{Re} f$ and $\operatorname{Im} f$ that determine the decrease in the echo signal at short times. Let us consider separately the cases of weak and strong electron-phonon interaction.

Weak interaction with phonons

The functions $\operatorname{Re} f$ and $\operatorname{Im} f$ decrease in absolute values as the interaction with the phonon becomes weaker. This follows from formulas (50) and (51). Consequently, the cosine in (60) and (61) is close to unity, and the echo signal behavior is determined primarily by the exponentials. This is illustrated in Figs. 4 and 5. The solid lines here represent echo signals calculated from (60) and (61) at $\tau/T_1=0$. The values of the function shown in Figs. 4 and 5 at the point $\tau=0$ are equal to $3f(0,T)$ and $2f(0,T)$, respectively. The Pekar–Huang factor $f(0,T)$ determines the strength of the linear electron-phonon interaction. It is related to the Debye–Waller factor α by the simple equation $\alpha=\exp[-f(0,T)]$. Consequently, the echo signal decay curve makes it possible to find the electron-phonon interaction strength. As the temperature increases the echo signal grows (see curves *2* in Figs. 4 and 5).

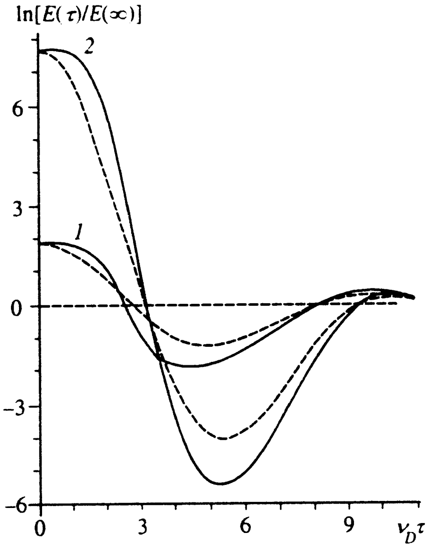

FIG. 4. Two-pulse echo signal decay for weak coupling calculated from Eqs. (60) (solid curves) and (65) (dashed curves). Here $kT/\hbar\nu_D=0$ (curve *1*) and 1 (curve *2*); $f(0,0)=0.625$.

The curves in Figs. 4 and 5 resemble the function $\operatorname{Re} f$ shown in Fig. 3. This suggests that the experimental curves for photon echo signal decay can be processed using the simpler formulas

$$\begin{aligned} R(\tau,0,\tau)&=\exp[3\operatorname{Re} f(\tau,T)-3f(0,T)],\\ R(\tau,t_w,\tau)&=\exp[2\operatorname{Re} f(\tau,T)-2f(0,T)]. \end{aligned} \tag{65}$$

Results obtained from the simplified formulas (65) are shown by dashed curves in Figs. 4 and 5. They are very close to the solid lines. Consequently, in the case of weak electron-

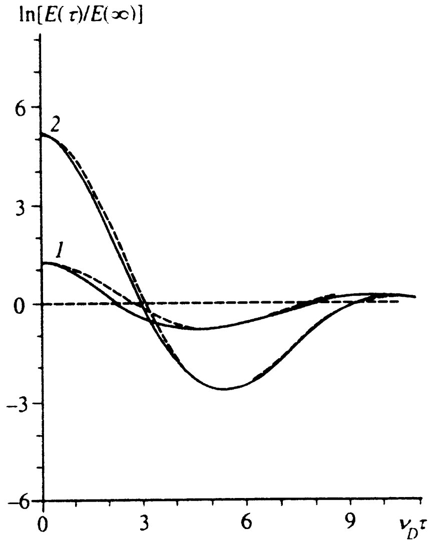

FIG. 5. Three-pulse echo signal decay for weak coupling calculated from Eqs. (61) (solid curves) and (65) (dashed curves); $Q=t_w/T_1=0$; $kT/\hbar\nu_D=0$ (curve *1*) and 1 (curve *2*); $f(0,0)=0.625$.

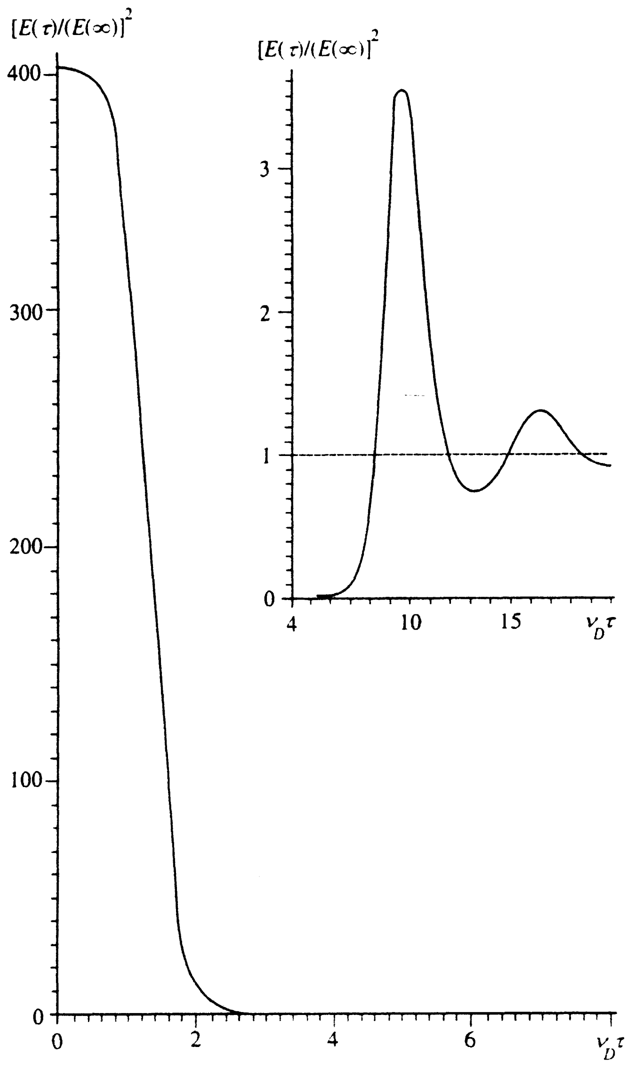

FIG. 6. Two-pulse echo signal decay for strong coupling calculated from Eq. (60); $kT/\hbar\nu_D=0$; $f(0,0)=1$.

phonon coupling, the logarithm of the photon echo signal decay curve nearly coincides in shape with the single-phonon function $\operatorname{Re} f(\tau,T)$ describing dipole phase decay. As for the optical band shape, according to formula (52) it is determined by both $\operatorname{Re} f(t,T)$ and $\operatorname{Im} f(t,T)$

$$I^{g,e}(\omega)=\frac{1}{\pi}\int_0^\infty dt\ \exp[\operatorname{Re} f(t,T)-f(0,T)]$$

$$\times\cos[(\omega-\omega_0)t\pm\operatorname{Im} f(t)], \qquad (66)$$

where "plus" and "minus" signs correspond to g and e. It follows from the Bloch optical equations that the photon echo decay function $E(\tau)$ and the optical band shape function $I(\omega)$ are related by Fourier transformation. For nonexponential decay of the signal in the range $\tau\nu_D<10$, there is no such a simple relation. This is demonstrated by formulas (60), (61), and (66).

Strong interaction with phonons

In this case, the function $\operatorname{Im} f(\tau)$ is large, and the preexponential factor in formulas (60) and (61) may therefore vanish several times. This is illustrated in Fig. 6. In this case the echo signal decreases rapidly down to a very small value and then exhibits very complicated behavior (see insert in Fig. 6). The region where the echo signal is particularly small contains zeros of the preexponential factor. We can see that in the case of strong coupling it becomes more difficult to extract information on the single-phonon function $f(\tau,T)$, but it is still possible. In this case, one should make use of the fact that the preexponential factor does not depend on temperature and therefore plays no part in considering the ratio of the signals measured at two different temperatures.

In conclusion, we should like to call attention to one important advantage of femtosecond echoes over other methods of selective spectroscopy, such as fluorescent line narrowing,[32] stable hole burning,[32] ordinary exponential echoes,[32] and spectroscopy of individual molecules.[33] All these methods are based on exciting an impurity center through its zero-phonon line. However, for strong electron-phonon interaction or near room temperature the Debye–Waller factor $\alpha=\exp[-f(0,T)]$ is very small, and the zero-phonon line is virtually absent. In this case all methods of selective spectroscopy are inapplicable, except femtosecond echoes. The femtosecond echo signal exists even when the zero phonon line is absent, because it has its origin in impurity centers excited through their phonon limb. This advantage of femtosecond echoes over other methods of selective spectroscopy is especially important in investigations of complex biologically important molecules, which must be studied in some cases without recourse to low temperatures.

The investigation described in this publication was made possible partly by grant No. Ph3-425-0909 of the International Science Foundation of G. Soros and partly by grant No. 94-02-03334-a of the Russian Foundation for Basic Research. The authors are grateful to these Foundations.

[1] E. L. Hahn, Phys. Rev. **80**, 580 (1950).
[2] U. Kh. Kopvillem and V. R. Nagibarov, Fizika Metallov i Metallovedenie **15**, 313 (1963).
[3] N. A. Kurnit, I. D. Abella, and S. R. Hartmann, Phys. Rev. Lett. **6**, 567 (1964).
[4] E. A. Manykin and V. V. Samartsev, *Optical Echo-Spectroscopy*, Nauka, Moscow (1984) [in Russian].
[5] U. H. Hesslink and D. A. Wiersma, in *Spectroscopy and Excitation Dynamics of Condensed Molecular Systems* (ed. V. M. Agranovich and R. M. Hochstrasser), North Holland, Amsterdam (1983).
[6] R. M. MacFarlane, R. M. Shelby, and R. L. Shoemaker, Phys. Rev. Lett. **43**, 1726 (1979).
[7] M. Berg, C. A. Walsh, L. R. Narasimhan *et al.*, J. Chem. Phys. **88**, 1564 (1988).
[8] W. B. Mims, K. Nassau, and J. D. McGee, Phys. Rev. **123**, 2059 (1961).
[9] R. Klauder and P. W. Anderson, Phys. Rev. **125**, 912 (1962).
[10] L. R. Narasimhan, K. A. Littau, D. W. Pack *et al.*, Chem. Rev. **90**, 439 (1990).
[11] H. C. Meijers and D. A. Wiersma, Phys. Rev. Lett. **68**, 381 (1992).
[12] P. C. Becker, H. L. Fragnito, J. Y. Bigot *et al.*, Phys. Rev. Lett. **63**, 505 (1989).
[13] J. Y. Bigot, M. T. Portella, R. W. Schoenlein *et al.*, Phys. Rev. Lett. **66**, 1138 (1991).
[14] S. Saikan, T. Nakabayashi, Y. Kanematsu, and N. Tato, Phys. Rev. **B38**, 7777 (1988).

[15] I. S. Osad'ko, Usp. Fiz. Nauk **128**, 31 (1979) [Sov. Phys. Usp. **22**, 311 (1979)].

[16] Y. R. Shen, *The Principles of Nonlinear Optics*, Wiley and Sons, N. Y. (1984).

[17] D. Bernhardt, P. Thomas, A. Weller *et al.*, Phys. Rev. **B43**, 8934 (1991).

[18] M. N. Belov and É. A. Manykin, Zh. Eksp. Teor. Fiz. **101**, 344 (1992) [Sov. Phys. JETP **74**, 182 (1992)].

[19] E. A. Manykin, I. Ya. Polishchuk, and A. L. Burin, Zh. Eksp. Teor. Fiz. **102**, 1629 (1992) [Sov. Phys. JETP **75**, 880 (1992)].

[20] M. Aihara, Phys. Rev. **B25**, 53 (1982).

[21] Yi. J. Yan and S. Mukamel, J. Chem. Phys. **94**, 179 (1991).

[22] L. E. Fried and S. Mukamel, Adv. Chem. Phys. **84**, 435 (1993).

[23] I. S. Osad'ko, Zh. Eksp. Teor. Fiz. **98**, 1045 (1990) [Sov. Phys. JETP **71**, 583 (1990)].

[24] I. S. Osad'ko and S. N. Gladenkova, Chem. Phys. Lett. **98**, 531 (1992).

[25] I. S. Osad'ko, J. Luminesc. **56**, 197 (1993).

[26] P. W. Anderson, B. I. Halperin, and C. M. Varma, Phil. Mag. **25**, 1 (1972).

[27] W. A. Phillips, J. Low Temp. Phys. **7**, 351 (1972).

[28] D. V. Donskoi, N. N. Zaitsev, and I. S. Osad'ko, Chem. Phys. **176**, 135 (1993).

[29] N. N. Zaitsev and I. S. Osad'ko, Zh. Eksp. Teor. Fiz. **104**, 4042 (1993) [Sov. Phys. JETP **77**, 950 (1993)].

[30] I. S. Osad'ko, in *Spectroscopy and Excitation Dynamics of Condensed Molecular Systems* (ed. V. M. Agranovich and R. M. Hochstrasser), North Holland, Amsterdam (1983).

[31] L. Allen and J. H. Eberly, *Optical Resonance and Two-Level Atoms*, Wiley and Sons, N. Y. (1975).

[32] I. S. Osad'ko, Adv. Polym. Sci. **114**, 123 (1994).

[33] M. Orrit, J. Bernard, and R. I. Personov, J. Phys. Chem. **97**, 10256 (1993).

Translated by A. M. Mozharovskii

This article was translated in Russia. It was reproduced here with all the stylistic changes by the Translation Editor and the Editor of the Russian text.